Note of Fast Runner

Ken

June, 2018*

1 About systems and methods

1.1 Requirements - system

- List assumptions
- Capture the required parameters (i.e. how to normalize the systems)
- – Resonance
  – nonlinear elastic components
  –

1.2 Requirements - method

- Applicable to complex system (e.g. for the designed mechanism)

1.3 ToDo

- Rearrange/updating references for fastRunner
- Check if the foot is sliding
- Check optimization tools ihmc have
  – parameter optimization tool using Gradient Decent or GA
- Ask Cris about the parameter range/selection

1.4 Questions

- Should I exclude the gyroscopic-based stabilization?
- Any solver for nonlinear program IHMC used?
- Any trajectory optimization method IHMC used?
- Methods to get stable Reciprocating Spoked Runner?

*Last update: June 18, 2018

2 Study

2.1 Jorge Cham's Dissertation - openloop control of 1DOF vertical hopper

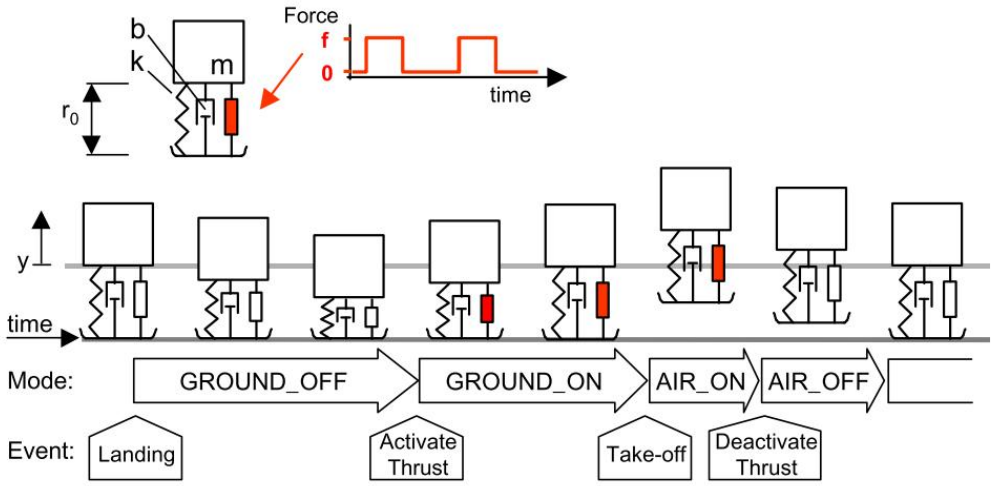

Figure 3-1. The vertical hopping model used for analysis. The hopper's leg consists of a spring, a damper and a force element which is active according to a binary motor pattern. The figure shows a sample trajectory of the hopper, the different modes that it goes through, and the events that trigger the transitions between the modes.

Figure 1: The schematic of a 1 DOF hopper [11]

2.1.1 System assumptions

- massless leg
- open-loop force control

2.1.2 Sequence

{AIR_OFF, GROUND_OFF, GROUND_ON, AIR_ON}

2.1.3 Equation of motion

Using the model as shown in Fig. 1, during the stand phase (i.e. $y \leq 0$), the equation of motion can be expressed as:

$$m\ddot{y} = -b\dot{y} + -ky - mg + f$$

where m is the mass, b is the damping, k is the stiffness, f is the control input. Normalized by weight, the equation becomes

$$\ddot{y} = -b/m\dot{y} + -k/my - g + f/m$$

Expressed in state space form:

$$\begin{bmatrix} \dot{y} \\ \ddot{y} \end{bmatrix} = \begin{bmatrix} 0 & 1 \\ -k/m & -b/m \end{bmatrix} \begin{bmatrix} y \\ \dot{y} \end{bmatrix} + \begin{bmatrix} 0 \\ -g + f/m \end{bmatrix} \tag{1}$$

or equivalently

$$\dot{X} = \begin{bmatrix} 0 & 1 \\ -\omega^2 & -2\xi\omega \end{bmatrix} X + \begin{bmatrix} 0 \\ -g + f_n(t) \end{bmatrix} = AX + B \tag{2}$$

where $X \triangleq [y, \dot{y}]^T$. When the hopper is in the air (i.e. $y > 0$, flight phase),

$$\dot{X} = \begin{bmatrix} 0 & 1 \\ 0 & 0 \end{bmatrix} X + \begin{bmatrix} 0 \\ -g \end{bmatrix} \tag{3}$$

Define the force of an open-loop motor pattern

$$f_n(t) = \begin{cases} f/m, & \text{if } t_{off} < t < t_{off} + t_{on}. \\ 0, & \text{otherwise.} \end{cases} \tag{4}$$

Solutions

For (3):

$$X(t) = \begin{bmatrix} 1 & t \\ 0 & 0 \end{bmatrix} X_0 + \begin{bmatrix} t^2/2 \\ t \end{bmatrix} (-g) \tag{5}$$

For (2) when actuator is on:

$$X(t) = e^{At}(X_0 - X_{eq_{on}}) + X_{eq_{on}} \tag{6}$$

For (2) when actuator is off:

$$X(t) = e^{At}(X_0 - X_{eq_{off}}) + X_{eq_{off}} \tag{7}$$

where $X_{eq_{on}}$ and $X_{eq_{off}}$ are the equilibrium states:

$$X_{eq_{on}} = [\frac{f_n - g}{\omega^2}, 0]^T \tag{8}$$

$$X_{eq_{off}} = [\frac{-g}{\omega^2}, 0]^T \tag{9}$$

2.1.4 Stability Analysis

Eigen values For (3), eigen values are ± 1, in inherently unstable. (Why this does not matter? Because the contact)

For (2), eigen values are $-\xi\omega \pm \omega\sqrt{(\xi^2 - 1)} = -\omega(\xi \pm \sqrt{\xi^2 - 1}) = -\omega(\xi \pm i\sqrt{1 - \xi^2})$ As long as $\omega$and $\xi$are larger than zero, the system is stable.

Poincare Method: The rest part skipped
Reasons: For more complex systems, hard to analytically derive the Poincare map (usually no closed-form solution). Found a package in spokeRunner simulation for Poincare Analysis (numerically), plan to reuse it.

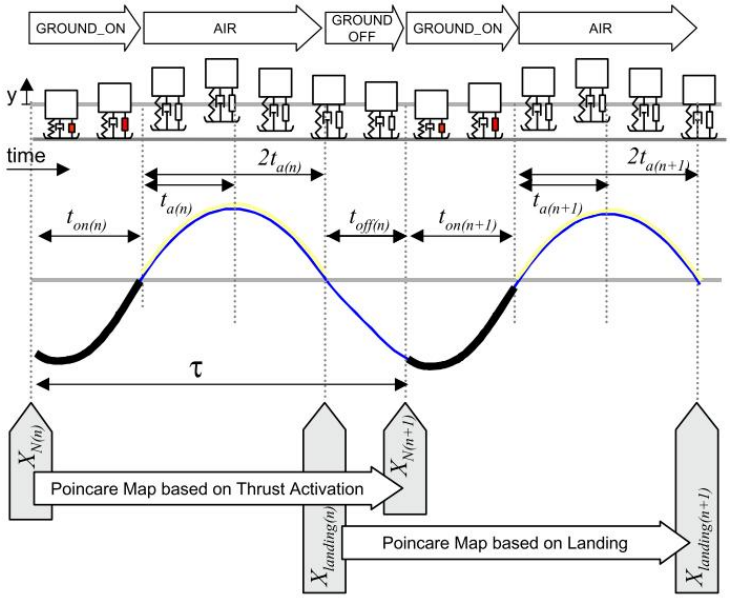

Figure 3-2. Illustration of a sample time history of the vertical hopper. The figure shows the two possibilities for formulating the Poincare Map used in analysis: a Map based on the state at thrust activation, and a Map based on the velocity and time at landing.

Figure 2: The modes of the hopper [11]

Assumptions:

- the period is T
- two modes need to be checked
- $X(0) = X_{N_n}$ where n indicates the n^{th} trajectory

Using Equations 6, we can derive

$$X(t_{on_n}) = e^{At_{on_n}}(X_{N_n} - X_{eq_{on}}) + X_{eq_{on}}$$

Use the fact that

$$X(t_{on_n} + 2t_{a_n}) = -X(t_{on_n})$$

Then we can calculate the $X_{N_{n+1}}$ as follows:

$$\begin{aligned} X_{N_{n+1}} &= e^{A(T-2t_{a_n}-t_{on_n})}(-X(t_{on_n}) - X_{eq_{off}}) + X_{eq_{off}} \\ X_{N_{n+1}} &= e^{A(T-2t_{a_n}-t_{on_n})}(-e^{At_{on_n}}(X_{N_n} - X_{eq_{on}}) - X_{eq_{on}}) - X_{eq_{off}}) + X_{eq_{off}} \\ &= X_{eq_{off}} - e^{A(T-2t_{a_n})}(X_{N_n} - X_{e_{on}}) - e^{A(T-2t_{a_n}-t_{on_n})}(X_{eq_{on}} + X_{eq_{off}}) \end{aligned} \tag{10}$$

About the second switch surface $X_{landing_n}$,

$$X_{landing_n} = -X(t_{on_n}) = -e^{At_{on_n}}(X_{N_n} - X_{eq_{on}}) - X_{eq_{on}} \tag{11}$$

2.2 Jerry's proof for pitch stability

3 Simulations

3.1 1 DOF Vertical Hopper with Open-loop Control[11]

System Setup

- body mass $m = 1$ with massless leg.
- $l = 1$
- $\omega_n = 30$
- $\xi = 0.15$ (or equivalently, $kp = 900, kd = 9$)
- static initial condition, COM height $= 0.3$
- open-loop force control:

$$f_n(t) = \begin{cases} f_n \in \mathbb{C}, & \text{if } t \in t_{on}. \\ 0, & \text{otherwise.} \end{cases}$$

- t_{on}: The duration of actuator activation, starts when the spring reaches the maximum compression, ends when the contact point leave the ground.

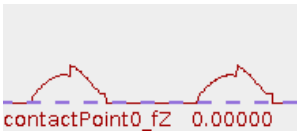

Figure 3: Ground reaction force when $f_n = 10$

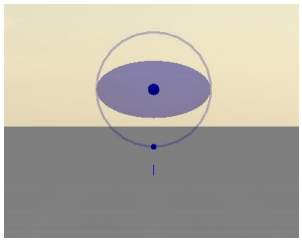

Figure 4: The vertical hopper, the blue dot at the bottom is the contact point of the massless leg.

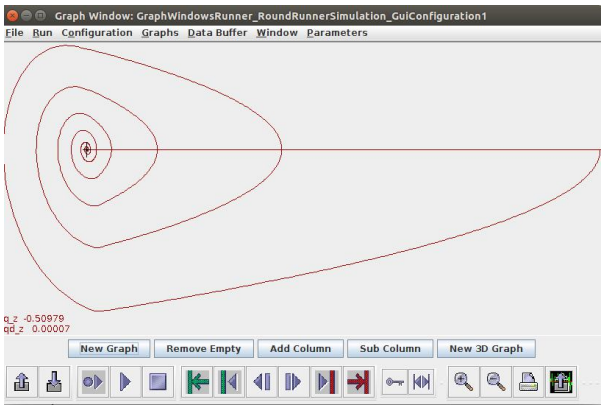

Figure 5: Phase portrait (stable spiral) of $f = 1$, period 0 sec

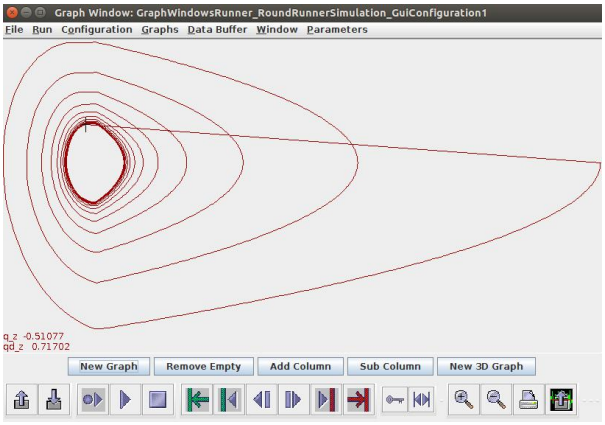

Figure 6: Phase portrait (stable limit cycle) of $f = 10$, period 0.27sec, (closer to the damped natural period ≈ 0.3295 sec)

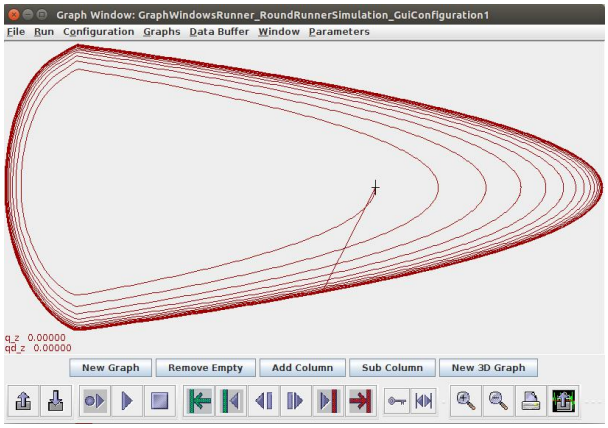

Figure 7: Phase portrait (stable limit cycle) of $f = 50$, period 0.859 sec

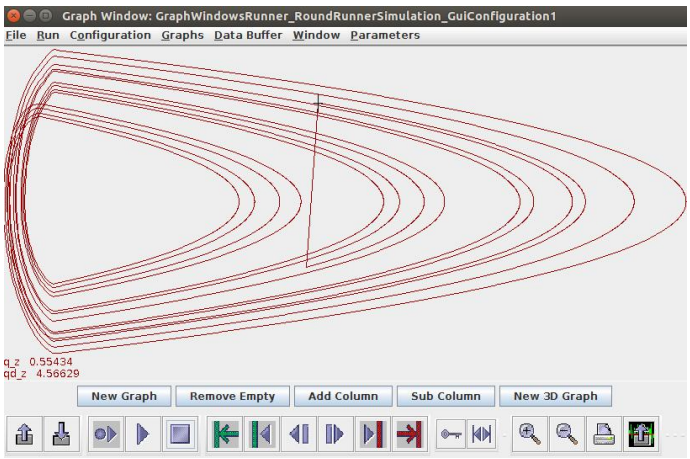

Figure 8: Phase portrait of $f = 100$, no stable limit cycle evolved (might be bifurcation).

4 Code implementation

4.1 Modeling and Parameters

Main idea: a virtual wheel (as the massless leg) with radius r_{wheel} penetrate the ground for a distance r_{pen} where a external force point pe is attached on it. A body (with mass m and inertia Iyy) is attached to the center of wheel. Using PD control to interpret contact force when p_e is under the ground.

06/07 First prototype (Not used now)

- Joint numbers: 2
- Joint types: Floating planer joint for virtual wheel and pin joint for the body link.
- Contact point type: External force point
- Virtual wheel rotation: set proper initial condition for virtual wheel (also need a large inertia to make it nearly constant).

Contact force: Assuming the ground height is 0,

$$F_z = kp(0 - pe_z) + kd(0 - ve_z) \tag{12}$$
$$\phi = atan2(pe_x, r_{wheel} - pe_z) \tag{13}$$
$$F_x = F_z tan(\phi) \tag{14}$$

where ve is the velocity vector of the contact point pe, kp and kd are the PD control parameters. F_x is calculated so that the vector of ground reaction force $[F_x, F_y, F_z]^T$ will point towards the virtual pivot (the center of the virtual wheel).

Assessments:

- Need to set a non-zero inertia of massless virtual wheel (for numerical stability), otherwise the simulation will diverge.
- The inertia of virtual wheel need to be a large one for constant rotational speed.
- Suggestions: remove the massless link, attach the external force point to the body and change its position in the controller every time step.

06/08 Round Runner

- Joint numbers: 1
- Joint types: Floating planer joint for the body link.
- Contact point type: External force point
- Virtual wheel rotation: Assigning the external force point location with respect to the joint in an open loop manner.
- Contact force: Assuming the ground height is 0,

$$F_z = kp(0 - pe_z) + kd(0 - ve_z) \tag{15}$$
$$\phi = atan2(pe_x, r_{wheel} - pe_z) \tag{16}$$
$$F_x = F_z tan(\phi) \tag{17}$$

where ve is the velocity vector of the contact point pe, kp and kd are the PD control parameters. F_x is calculated so that the vector of ground reaction force $[F_x, F_y, F_z]^T$ will point towards the virtual pivot (the center of the virtual wheel).

Assessments:

- The ground reaction force looks better, while the energy is not balanced (after a while it will move towards the negative x direction)
- The inertia of virtual wheel need to be a large one for constant rotational speed.
- Suggestions: Use the ground contact point (instead of external force point) to see how it goes.

06/11 Round Runner(with Ground Contact Point)

- Joint numbers: 1
- Joint types: Floating planer joint for the body link.
- Contact point type: Ground contact point, linear contact model[1]
- Virtual wheel rotation: Assigning the external force point location with respect to the joint in an open loop manner.
- **Contact point number** Parameterized, currently set to 3-6 points.
- Contact force: using built-in functionalities, only assigning the kp, kd (PD parameters in the z direction), kp_x, and kd_x (PD parameters in the x/y directions).

Assessments:

- Was able to generate a stable walking. Contact point has sliding.
- Due to setting up stiffness and damping for x and z separately, the force is not always point towards the virtual pivot.

06/12 Round Runner(with External Contact Point Point)

- Implement the same one as 06/11, but replace the ground contact point to the external one (because it is more complex for ground contact point to adjust stiffness/damping as parameters.)
- implement the linear ground contact model basically.

06/13 Round Runner

- Parameterize contact point numbers
- Adding enum for switching between different setup: contact point type and the corresponding ground reaction force calculation: (w.r.t to the world frame or inertia frame.)

06/16 Round Runner (vertical hopper)

- Adding vertical hopper with open-loop force control
- Playing with open-loop force magnitudes for different stability conditions

[1]Disable the hardening stiffness in z direction by setting groundStiffeningLength to Double.NEGATIVE_INFINITY

5 Info might be useful

5.1 Going through references

1. Compare different terrestiral locomotions: Some parameters of the walk are not speed- dependent. The swing duration is a constant time parameter [1].
2. Trunk plays an important role during walking (birds) [2].
3. The use of these drives (Resonance drives, with adaptive control) allows increasing machine's quickness several times and decreasing energy expenses simultaneously 10-50 times [3].
4. Light weight leg (ostrich vs. moa) can run faster[5]. Also a famous allometric equation:

$$Y = M^{3/4} \tag{18}$$

   where M is the body mass, Y is the metabolic rate.
5. Human's walking may not be really self-optimized: the preferred speed maybe different from the energetically optimal speed[8].
6. It is concluded that the most important adjustment to the bodys spring system to accommodate higher stride frequencies is that leg spring becomes stiffer [19].
7. magic equations for imd force (ostrich) [26]
8. gait frequency was reported to be highly correlated with the resonant frequency of the mass-spring model [30]
9. WABIAN, why you are here? [31]

5.2 Categories

1. Nonlinear oscillators/components [3, 6, 9, 10, 12, 28, 39];
2. zoology, biomechanics of animals: [1, 2, 4, 5, 16]
3. Bio-inspired robots: [7, 32]
4. Reference I should read: [11, 15, 27, 28]
5. Article not found (or not free)[4].
6. Robots in 3D: [13]
7. Stability analysis (Monocycle, linearized system) [14] (Limit cycle) [11, 27] dimensionless [41]
8. Biology/Anatomical structure [17, 20]
9. Light weight fast robot [18, 25]
10. take a look again [21]
11. mechanism design of robot [22]
12. quadruped reference [23] MIT Cheetah[37]
13. human energy cost, resonance usage [24, 8, 38, 40]
14. walking parameterization [29, 21, 42]
15. human-animal differences [15]
16. open-loop robot [33], passive robot [35, 34, 36]

References

[1] Anick Abourachid. Kinematic parameters of terrestrial locomotion in cursorial (ratites), swimming (ducks), and striding birds (quail and guinea fowl). *Comparative Biochemistry and Physiology Part A: Molecular and Integrative Physiology*, 131(1):113–119, dec 2001.

[2] Anick Abourachid, Remi Hackert, Marc Herbin, Paul A. Libourel, François Lambert, Henri Gioanni, Pauline Provini, Pierre Blazevic, and Vincent Hugel. Bird terrestrial locomotion as revealed by 3D kinematics. *Zoology*, 114(6):360–368, dec 2011.

[3] T. Akinfiev and M. Armada. Elements of built-in diagnostics for resonance drive with adaptive control system. In *International Symposium on Automation and Robotics in Construction*, pages 617–621, Madrid, Spain, 1999.

[4] R. Mc N Alexander, G. M O Maloiy, R. Njau, and A. S. Jayes. Mechanics of running of the ostrich (Struthio camelus). *Journal of Zoology*, 187(2):169–178, 1979.

[5] R. McNeill Alexander. The legs of ostriches (Struthio) and moas (Pachyornis). *Acta Biotheoretica*, 34(2-4):165–174, 1985.

[6] G. V. Anand. Nonlinear Resonance in Stretched Strings with Viscous Damping. *The Journal of the Acoustical Society of America*, 40(6):1517–1528, 1966.

[7] Arvind Ananthanarayanan, Mojtaba Azadi, and Sangbae Kim. Towards a bio-inspired leg design for high-speed running. *Bioinspiration and Biomimetics*, 7(4):046005, dec 2012.

[8] Elizabeth Arnall, Jessica Pyatt, Chelsie Rice, Katie L Anderson, and Duncan Mitchell. Resonance in Human Walking Economy: How Natural Is It? *International Journal of Undergraduate Research and Creative Activities*, 4(1), 2012.

[9] V. I. Babitsky and M. Y. Chitayev. Adaptive high-speed resonant robot. *Mechatronics*, 6(8):897–913, dec 1996.

[10] Jonas Buchli, Fumiya Iida, and Auke Jan Ijspeert. Finding resonance: Adaptive frequency oscillators for dynamic legged locomotion. In *IEEE International Conference on Intelligent Robots and Systems*, pages 3903–3909, Beijing, China, 2006.

[11] J. G. Cham. *On Performance and Stability in Open-Loop Running*. PhD thesis, Stanford University, 2002.

[12] S. Chatterjee and Anindya Malas. On the stiffness-switching methods for generating self-excited oscillations in simple mechanical systems. *Journal of Sound and Vibration*, 331(8):1742–1748, apr 2012.

[13] Michael J. Coleman, Anindya Chatterjee, and Andy Ruina. Motions of a rimless spoked wheel: a simple three-dimensional system with impacts. *Dynamics and Stability of Systems*, 12(3):139–159, 1997.

[14] Michael J. Coleman and Jim M. Papadopoulos. Intrinsic stability of a classical monocycle and a generalized monocycle. In *Bicycle and Motorcycle Dynamics, Symposium on Dynamics and Control of Single Track Vehicles*, Delft, Netherlands, 2010.

[15] M. A. Daley and A. A. Biewener. Running over rough terrain reveals limb control for intrinsic stability. *Proceedings of the National Academy of Sciences*, 103(42):15681–15686, oct 2006.

[16] M. A. Daley, G. Felix, and A. A. Biewener. Running stability is enhanced by a proximo-distal gradient in joint neuromechanical control. *Journal of Experimental Biology*, 210(3):383–394, feb 2007.

[17] T. El-Mahdy, S. M. El-Nahla, L. C. Abbott, and S. A.M. Hassan. Innervation of the pelvic limb of the adult ostrich (Struthio camelus). *Journal of Veterinary Medicine Series C: Anatomia Histologia Embryologia*, 39(5):411–425, 2010.

[18] Darrell Ethington. Dash Robotics Reveals A DIY High-Speed Running Robot Kit, Which Hobbyists Can Own For Just $65, 2013.

[19] Claire T. Farley and Octavio González. Leg stiffness and stride frequency in human running. *Journal of Biomechanics*, 29(2):181–186, 1996.

[20] D. Gangl, G. E. Weissengruber, M. Egerbacher, and G. Forstenpointner. Anatomical description of the muscles of the pelvic limb in the ostrich (Struthio camelus). *Journal of Veterinary Medicine Series C: Anatomia Histologia Embryologia*, 33(2):100–114, 2004.

[21] S. M. Gatesy and A. A. Biewener. Bipedal locomotion: effects of speed, size and limb posture in birds and humans. *Journal of Zoology*, 224(1):127–147, 1991.

[22] Martin Grimmer and André Seyfarth. Design of a Series Elastic Actuator driven ankle prosthesis : The trade-off between energy and peak power optimization. In *Dynamic Walking*, 2011.

[23] R Hackert, H Witte, and M S Fischer. Interactions between motions of the trunk and the angle of attack of the forelimbs in synchronous gaits of the pika (Ochotona rufescens). In *Adaptive Motion of Animals and Machines*, pages 69–77. Springer, 2006.

[24] Kenneth G. Holt, Joseph Hamill, and Robert O. Andres. Predicting the minimal energy costs of human walking. *Medicine & Science in Sports & Exercise*, 23(4):491–498, 1991.

[25] Fumiya Iida, Murat Reis, Nandan Maheshwari, Xiaoxiang Yu, and Amir Jafari. Toward efficient, fast, and versatile running robots based on free vibration. In *Dynamic Walking*, Pensacola, FL, 2012.

[26] D. L. Jindrich, N. C. Smith, K. Jespers, and A. M. Wilson. Mechanics of cutting maneuvers by ostriches (Struthio camelus). *Journal of Experimental Biology*, 210(8):1378–1390, 2007.

[27] Takahiro Kagawa and Yoji Uno. Necessary condition for forward progression in ballistic walking. *Human Movement Science*, 29(6):964–976, dec 2010.

[28] Jg Daniël Karssen and Martijn Wisse. Running with improved disturbance rejection by using non-linear leg springs. *International Journal of Robotics Research*, 30(13):1585–1595, sep 2011.

[29] Leng Feng Lee and Venkat N. Krovi. Musculoskeletal simulation-based parametric study of optimal gait frequency in biped locomotion. In *International Conference on Biomedical Robotics and Biomechatronics*, pages 354–359, Scottsdale, AZ, 2008.

[30] Myunghyun Lee, Seyoung Kim, and Sukyung Park. Leg stiffness increases with load to achieve resonance-based CoM oscillation. In *Dynamic Walking*, Pittsburgh, PA, 2013.

[31] Hun-ok Lim, Y Ogura, Atsuo Takanishi, and Proc R Soc A. Locomotion pattern generation and mechanisms of a new biped walking machine. *Proceedings of the Royal Society of London A: Mathematical and Physical Sciences*, 464(2089):273–288, 2008.

[32] R. J. Lock, S. C. Burgess, and R. Vaidyanathan. Multi-modal locomotion: From animal to application. *Bioinspiration and Biomimetics*, 9(1), dec 2014.

[33] Katja Mombaur, H Georg Bock, Johannes Schlöder, and Richard Longman. Stable Walking and Running Robots Without Feedback. In *Climbing and Walking Robots*, pages 725–735. 2005.

[34] Dai Owaki, Masatoshi Koyama, Shin'ichi Yamaguchi, Shota Kubo, and Akio Ishiguro. A two-dimensional passive dynamic running biped with knees. In *Proceedings - IEEE International Conference on Robotics and Automation*, pages 5237–5242, 2010.

[35] Dai Owaki, Masatoshi Koyama, Shin'Ichi Yamaguchi, Shota Kubo, and Akio Ishiguro. A 2-D passive-dynamic-running biped with elastic elements. *IEEE Transactions on Robotics*, 27(1):156–162, 2011.

[36] Dai Owaki, Koichi Osuka, and Akio Ishiguro. Understanding the common principle underlying passive dynamic walking and running. *2009 IEEE/RSJ International Conference on Intelligent Robots and Systems, IROS 2009*, pages 3208–3213, 2009.

[37] Hae-won Park, Sangbae Kim, and Our Approach. Variable Speed Galloping Control using Vertical Impulse Modulation for Quadruped Robots : Application to MIT Cheetah Robot Click for Video Overview, 2012.

[38] Sukyung Park. Can human walking be mimicked by resonance-based oscillation? In *The 7th World Congress on Biomimetics, Artificial Muscles and Nano-Bio*, volume 44, page 2013, Jeju Island, South Korea, 2013.

[39] M C Plooij and M Wisse. A spring mechanism for resonant robotic arms. In *Workshop on Human Friendly Robotics*, page 5, 2011.

[40] V. Racic, A. Pavic, and J. M.W. Brownjohn. Experimental identification and analytical modelling of human walking forces: Literature review. *Journal of Sound and Vibration*, 326(1-2):1–49, sep 2009.

[41] Sebastian Riese and Andre Seyfarth. Stance leg control: Variation of leg parameters supports stable hopping. *Bioinspiration and Biomimetics*, 7(1):016006, mar 2012.

[42] Robert E Weems. Locomotor Speeds and Patterns of Running Behavior in Non-Maniraptoriform Theropod Dinosaurs. *New Mexico Museum of Natural History and Science Bulletin*, 37:379–389, 2006.